

SUPPLEMENTAL FIG.LEGENDS

Fig.S1: Generation of FKBP^{degron} lines. (Related to Fig.1)

- (A) Outline of protocol used to generate RAD21 and WAPL-FKBP^{degron} mESCs
- (B) PCR amplifying knock-in site of parental TST mESC lines (WT) and RAD21 and WAPL-FKBP^{degron} clones. One PCR primer was located outside of the homology arms to ensure that only the endogenous locus was amplified. FKBP^{degron} tag is ~400bp.
- (C) Western blots for RAD21 and GADPH loading control in RAD21-FKBP^{degron} lines at day 7 of differentiation. Samples treated with DMSO vehicle control (D) or 500nM dTAG-13 (13).
- (D) Western blots for WAPL and GADPH loading control in WAPL-FKBP^{degron} lines at day 7 of differentiation. Samples treated with DMSO vehicle control (D) or 500nM dTAG-13 (13).
- (E) Sanger sequencing of RAD21-FKBP^{degron} and WAPL-FKBP^{degron} lines.
- (F) Comparison of genomic DNA (input DNA) in WAPL-FKBP^{degron} lines at chromosome 14. Sharp dip in WAPL-FKBP^{degron}, clone H7 input corresponds to the end of the right 900bp homology arm used for knock-in of the tag. Reads mapping to the plasmid backbone used for the homology repair template were also found here, although they did not appear to be incorporated into the main Wapl transcript.
- (G) Immunofluorescence of WAPL-HA in WAPL-FKBP^{degron} lines at day 7 of differentiation. Samples treated with DMSO vehicle control (D) or 500nM dTAG-13 (13).

Fig.S2: Cell cycle profiling of FKBP^{degron} lines. (Related to Fig.1)

- (A) DNA content profiles via propidium iodide staining of RAD21-FKBP^{degron} lines at day 7 of differentiation. Samples treated with DMSO vehicle control (D) or 500nM dTAG-13 (13) as indicated.
- (B) DNA content profiles via propidium iodide staining of RAD21-FKBP^{degron} lines at day 10 of differentiation.
- (C) DNA content profiles via propidium iodide staining of WAPL-FKBP^{degron} lines at day 7 of differentiation.
- (D) DNA content profiles via propidium iodide staining of WAPL-FKBP^{degron} lines at day 7 of differentiation.
- (E) DNA content profiles via propidium iodide staining of WAPL-FKBP^{degron} lines at day 10 of differentiation.

Fig.S3. Replication of architectural changes across FKBP^{degron} clones. (Related to Fig. s 1 and 2)

- (A) Metaplot and heatmap of RAD21 binding by cChIP-seq in WAPL-FKBP^{degron} clone H2.
- (B) Frequency versus distance plots for Hi-C interaction maps across individual FKBP^{degron} clones at all time points used in this study. Samples treated with DMSO vehicle control 500nM dTAG-13 as indicated. Saddle plot analysis of compartment strength in RAD21-FKBP^{degron} Hi-C maps at day 7 (clones merged) also shown. Scores represent B-B, B-A, and A-A compartment interaction strength. Representative sections of day 7 Hi-C maps at different resolutions for RAD21-FKBP^{degron} clones.
- (C) Representative sections of day 10 Hi-C maps at different resolutions for RAD21-FKBP^{degron} clones.
- (D) Section of day 7 RAD21-FKBP^{degron} Hi-C maps (clones merged) displaying example of cohesin-independent loops not anchored by H3K27me3 (arrows).
- (E) Representative sections of day 7 Hi-C maps at different resolutions for WAPL-FKBP^{degron} clones.
- (F) Aggregate Peak Analysis plots of aggregate RAD21-FKBP^{degron} Hi-C signal at day 7 (clones merged) over regions anchored by Hox clusters.
- (G) Aggregate Peak Analysis plots of aggregate RAD21-FKBP^{degron} Hi-C signal at day 10 (clones merged) over regions anchored by Hox clusters.
- (H) Aggregate Peak Analysis plots of aggregate WAPL-FKBP^{degron} Hi-C signal at day 7 (clones merged) over regions anchored by Hox clusters.

Fig.S4: Additional analysis of cChIP after short term WAPL degradation and gene expression changes after 3 day degradation. (Related to Fig.3)

- (A) Log2-fold (dTAG-13/DMSO) change in FKBP^{degron} lines of genes overlapping RAD21-bound anchors of loops. Loops called in respective DMSO control samples. Significant p-values by Wilcoxon rank test indicated by * ($p < 2.772e-06$). N.S., not significant.
- (B) Metaplot and heatmaps of RAD21 binding by H3K27me3 cChIP-seq after 8 hours of WAPL degradation genome-wide (left) and on the active X chromosome (right).
- (C) Metaplot and heatmaps of RAD21 binding by H3K27me3 cChIP after 8 hours of WAPL on the centromeric 30Mb, middle 100Mb, and telomeric 30Mb of the inactive X chromosome.

- (D) Tracks of H3K27me3 by cChIP-seq on the X chromosome after 8 hours of WAPL degradation or DMSO control treatment. Log fold ratio tracks (dTAG-13/DMSO) are also shown (Δ).
- (E) Genes upregulated or downregulated upon WAPL degradation from days 7-10 (relative to DMSO control) overlapping with H3K27me3 cChIP-seq peaks. All genes shown for reference.
- (F) RNA-seq and H3K27me3 ChIP-seq over the *Usp17* and *Zscan4* gene clusters in CTCF-AID degron lines after 4 days of auxin treatment or untreated cells (Nora et al., 2017) or after 3 days of DMSO or dTAG-13 treatment (500nM) in WAPL-FKBP^{degron} cells early in differentiation (days 4-7). Note that cohesin was recently implicated in regulation of such 2-cell genes (Zhang et al., 2020).

Fig.S5. Cohesin significantly contributes to proper upregulation of proximal super-enhancer targets without affecting long-range super-enhancer interactions.

- (A) Distance to nearest super-enhancer (Whyte et al. 2013) for expressed genes upregulated or downregulated upon RAD21 degradation (relative to DMSO). Expressed genes shown for reference. Significant p-values by Wilcoxon rank test indicated by * ($p<0.006057$), ** ($p<0.01569$). N.S., not significant.
- (B) Day 7 RAD21-FKBP^{degron} PRO-seq and RAD21 cChIP-seq signal over representative super-enhancer targets downregulated upon 8 hours RAD21 degradation (relative to DMSO).
- (C) Aggregate Peak Analysis plots of aggregate RAD21-FKBP^{degron} Hi-C signal (clones merged) over regions anchored by super-enhancers. Super-enhancers segregated by distance into 5 quantiles.

Fig.S6. Additional biological replicate for Xist CHART-seq and H3K27me3 cChIP-seq to examine spreading defects. (Related to Fig.6).

- (A) Tracks of CHART-seq (Xist) and H3K27me3 cChIP-seq over the X chromosome and allelic RAD21 cChIP over the Xa and Xi in WAPL-FKBP^{degron} lines treated from days 4-7 of differentiation with DMSO (D) or 500nM dTAG-13 (13). Log fold ratio tracks (dTAG-13/DMSO) are also shown (Δ). Principal component corresponding to compartments on

the Xi in same samples shown for reference (PC1). Hi-C contacts to the 1Mb bin containing the Xist transcription locus in same conditions also shown.

- (B) Boxplot showing Xist coverage over 100kb bins in the centromeric most 30Mb, middle 100Mb, and telomeric most 30Mb of the X chromosome in WAPL-FKBP^{degron} lines treated as in (A). Significant p-values by Wilcoxon signed rank test indicated by * ($p<2.2e-16$).
- (C) Boxplots showing allelic H3K27me3 coverage over 100kb bins in the centromeric most 30Mb, middle 100Mb, and telomeric most 30Mb of the X chromosome in WAPL-FKBP^{degron} lines treated as in (A). Significant p-values by Wilcoxon signed rank test indicated by * ($p<2.2e-16$), ** ($p<0.03$), and *** ($p<2.2e-05$). N.S., not significant.
- (D) Boxplot showing average Xist density over different classes of genes on the X chromosome in WAPL-FKBP^{degron} lines treated as in (A). Significant p-values by Wilcoxon signed rank test indicated by * ($p<2.2e-16$) and ** ($p<1.049e-14$). N.S., not significant.
- (E) Boxplot showing average allelic H3K27me3 density over different classes of genes on the X chromosome in WAPL-FKBP^{degron} lines treated as in (A). Significant p-values by Wilcoxon signed rank test indicated by * ($p<2.2e-16$), ** ($p<2.79e-15$), *** ($p<9.04e-13$), **** ($p<0.001573$), ***** ($p<0.001954$), ***** ($p<2.239e-05$), ***** ($p<1.308e-05$). N.S., not significant.
- (F) Boxplot showing Xist average density over 100kb bins in S1 and S2 compartments. Significant p-values by Wilcoxon signed rank test indicated by * ($p<2.2e-16$) and ** ($p<4.13e-09$).
- (G) Boxplot showing average allelic H3K27me3 density over 100kb bins in S1 and S2 compartments. Significant p-values by Wilcoxon signed rank test indicated by * ($p<2.2e-16$), **($p<0.0082$), *** ($p<0.005$), ****($p<1.86e-10$), ***** ($p<1.89e-08$), ***** ($p<2.127e-05$), ***** ($p<0.0008859$).
- (H) Boxplots showing average Xist and allelic H3K27me3 density over 100kb within 10Mb of the Xist transcription locus. Significant p-values by Wilcoxon signed rank test indicated by * ($p<1.543e-05$), **($p<4.026e-13$).

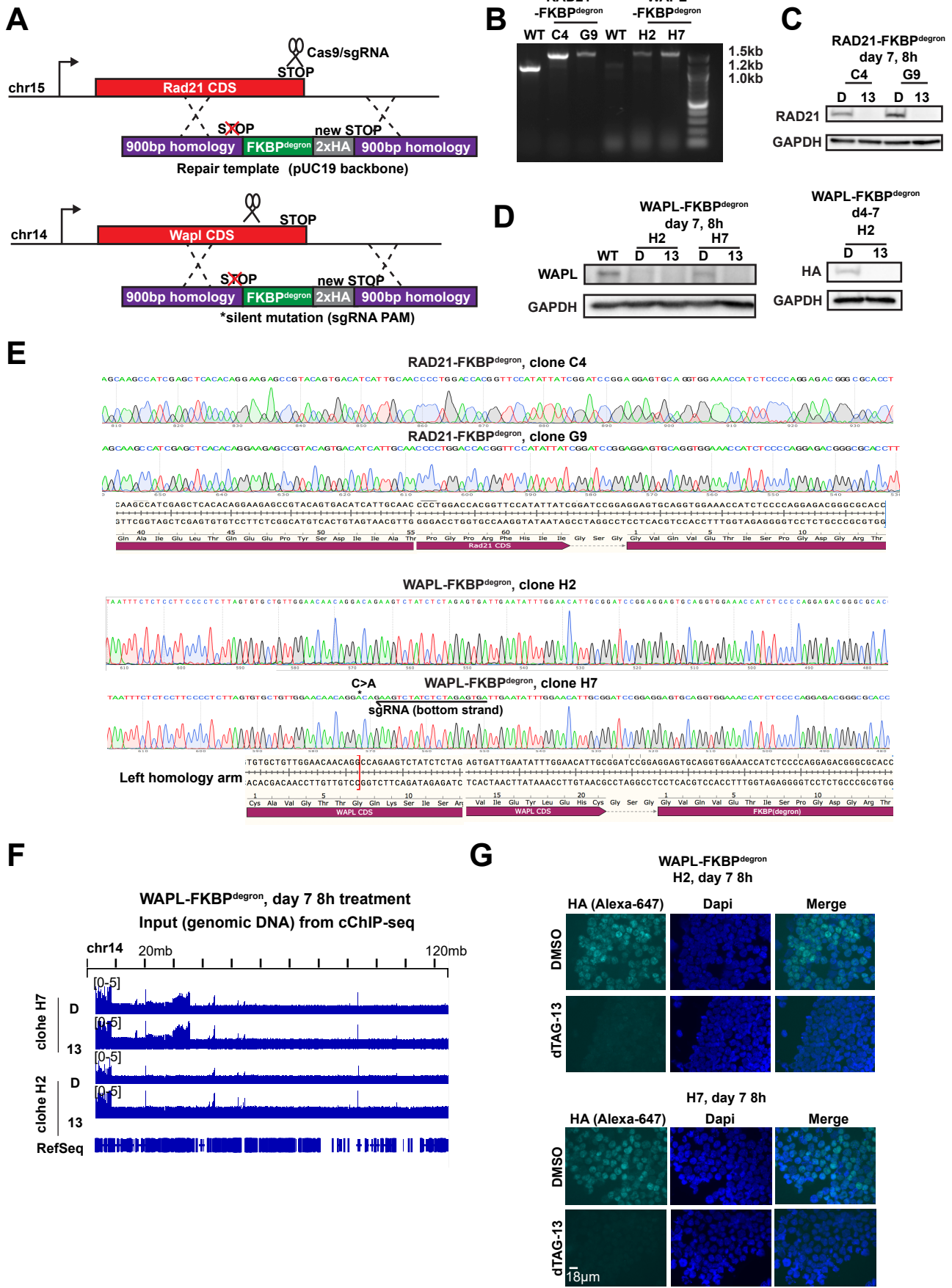


Figure S1

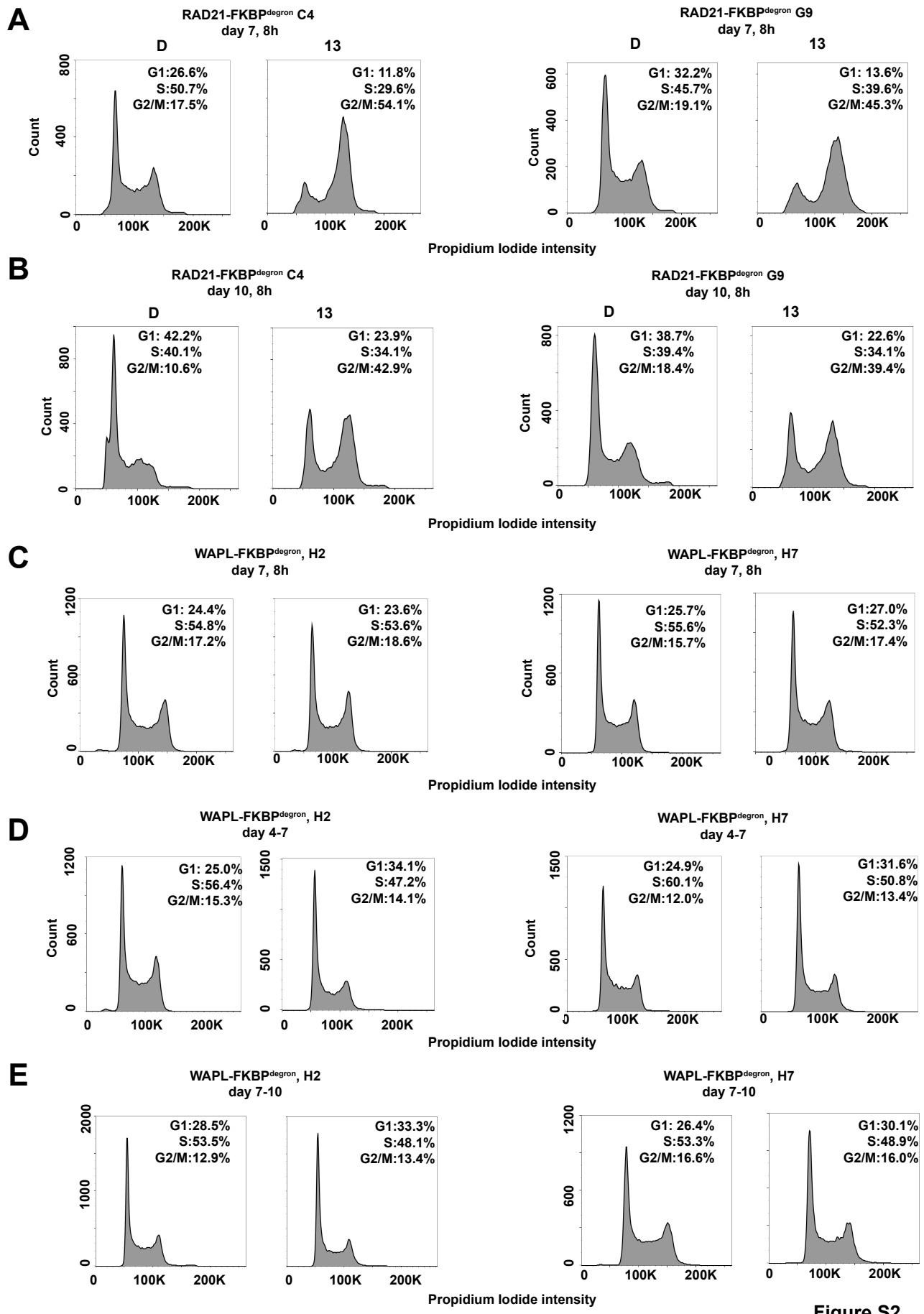


Figure S2

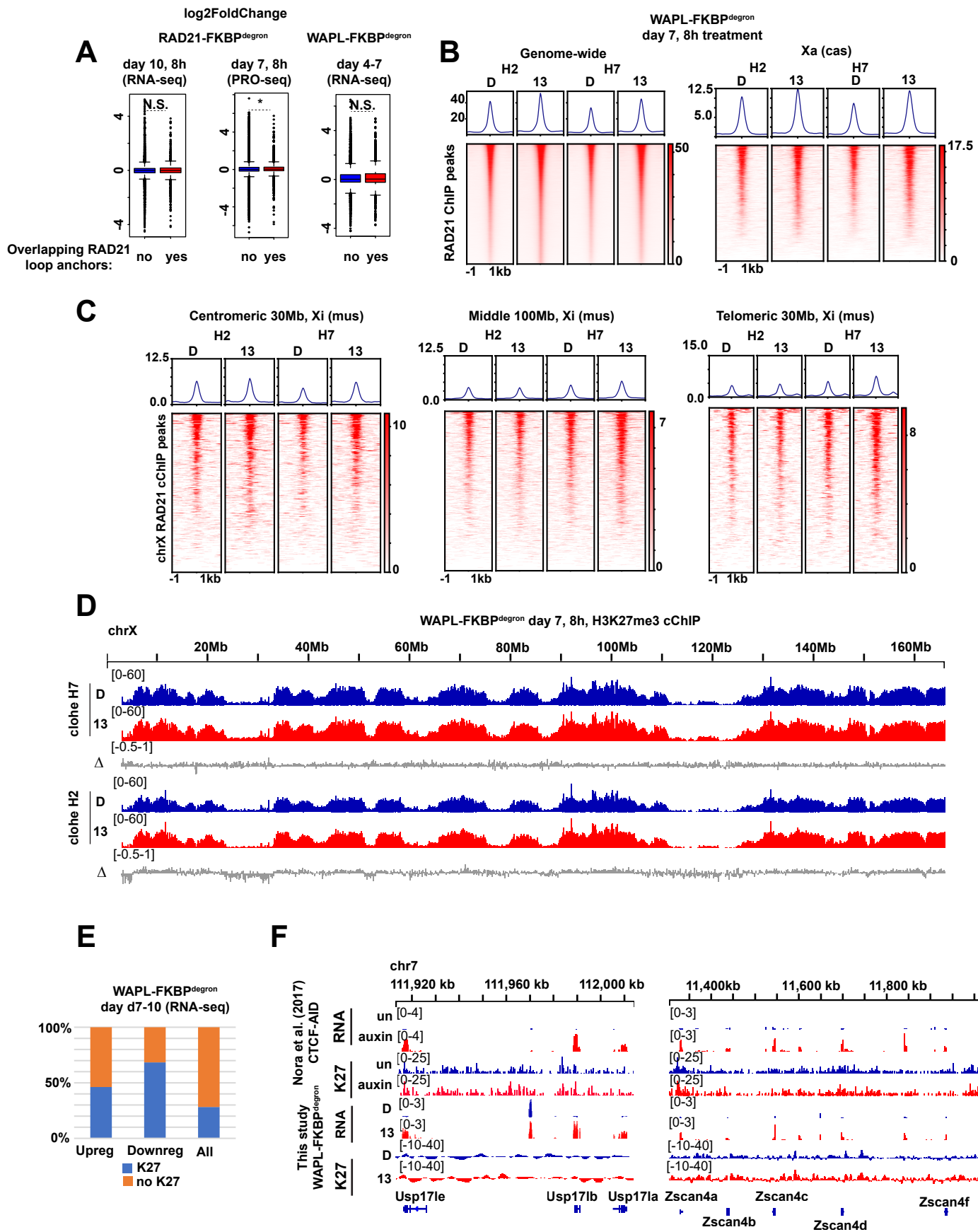


Figure S4

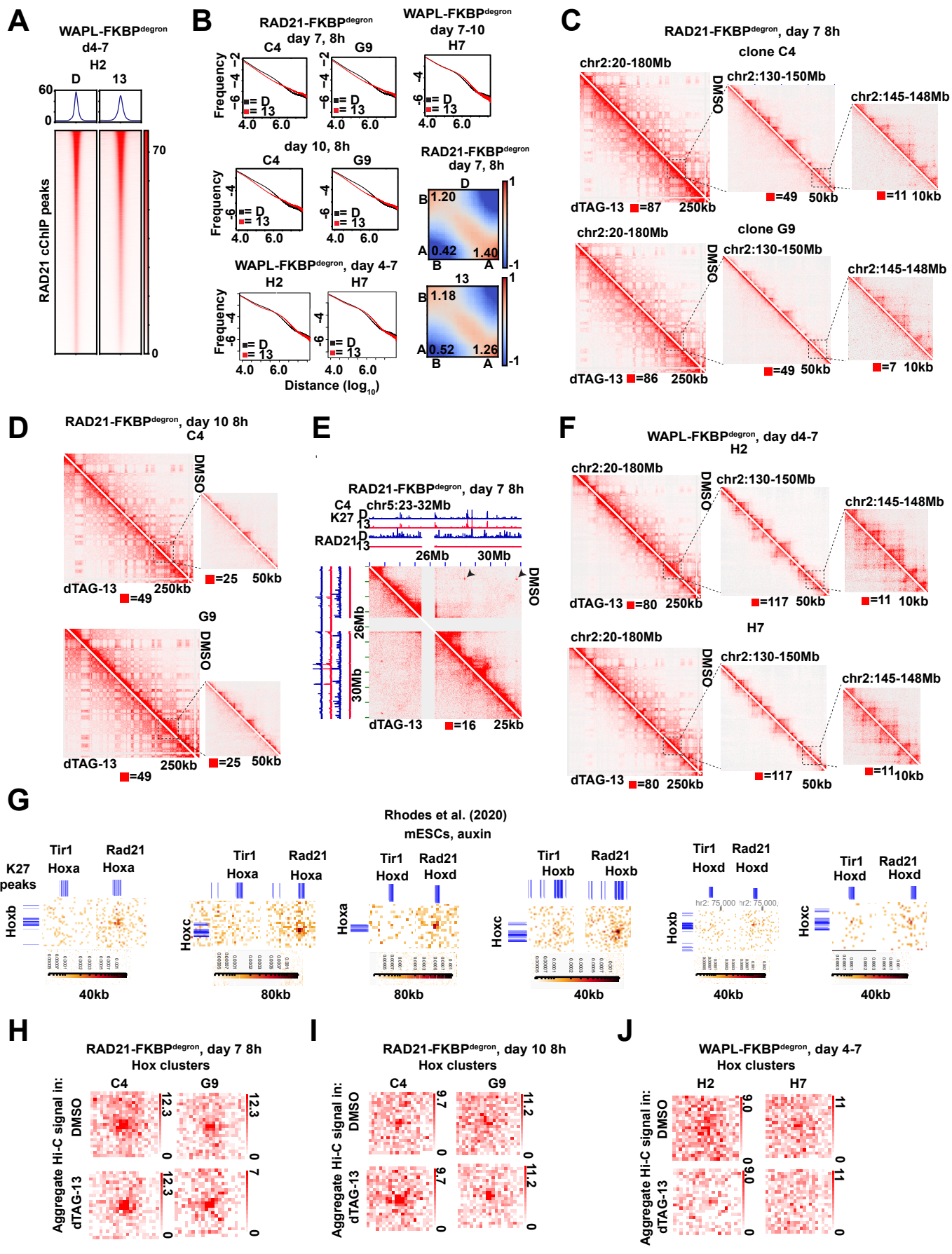


Figure S3

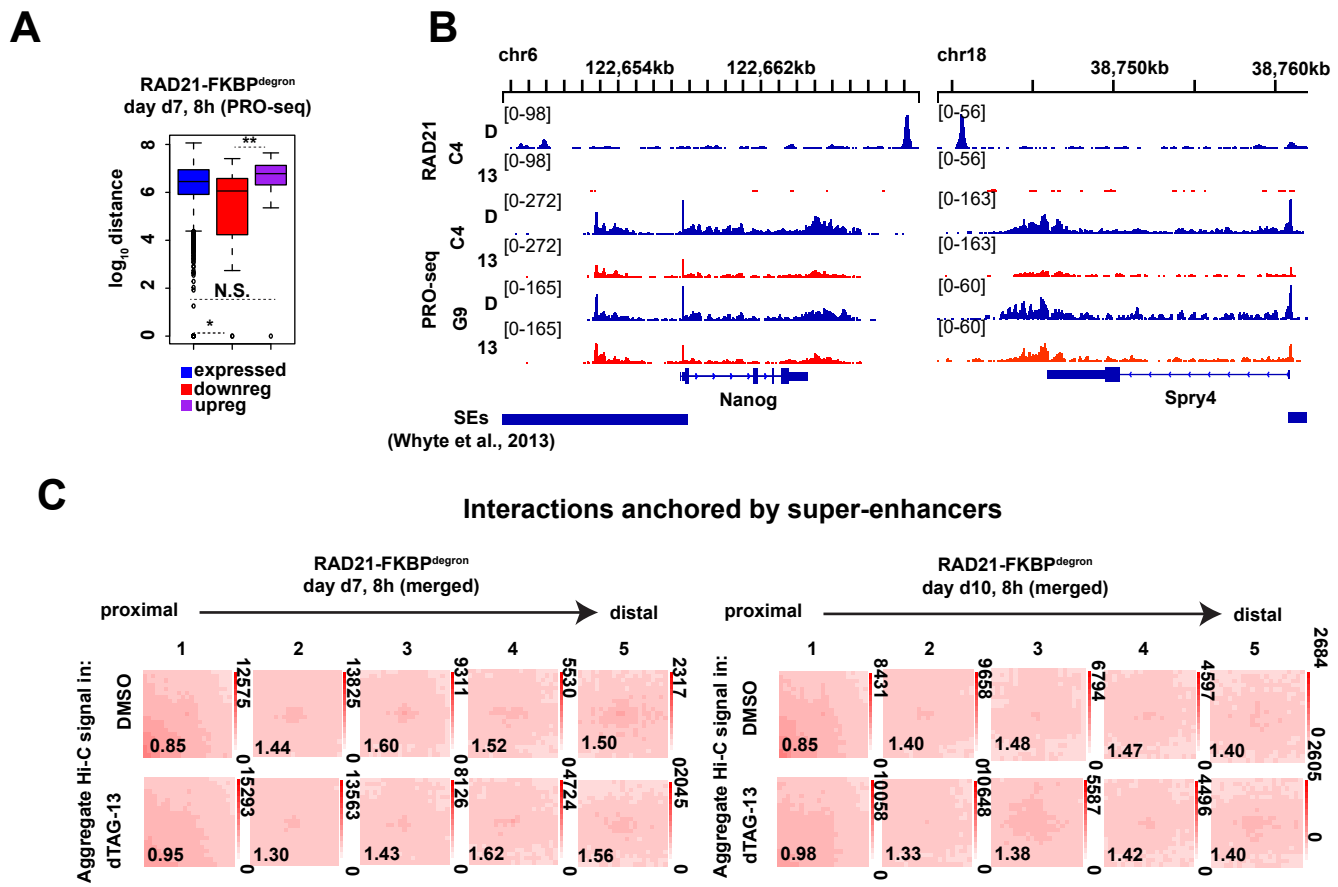


Figure S5

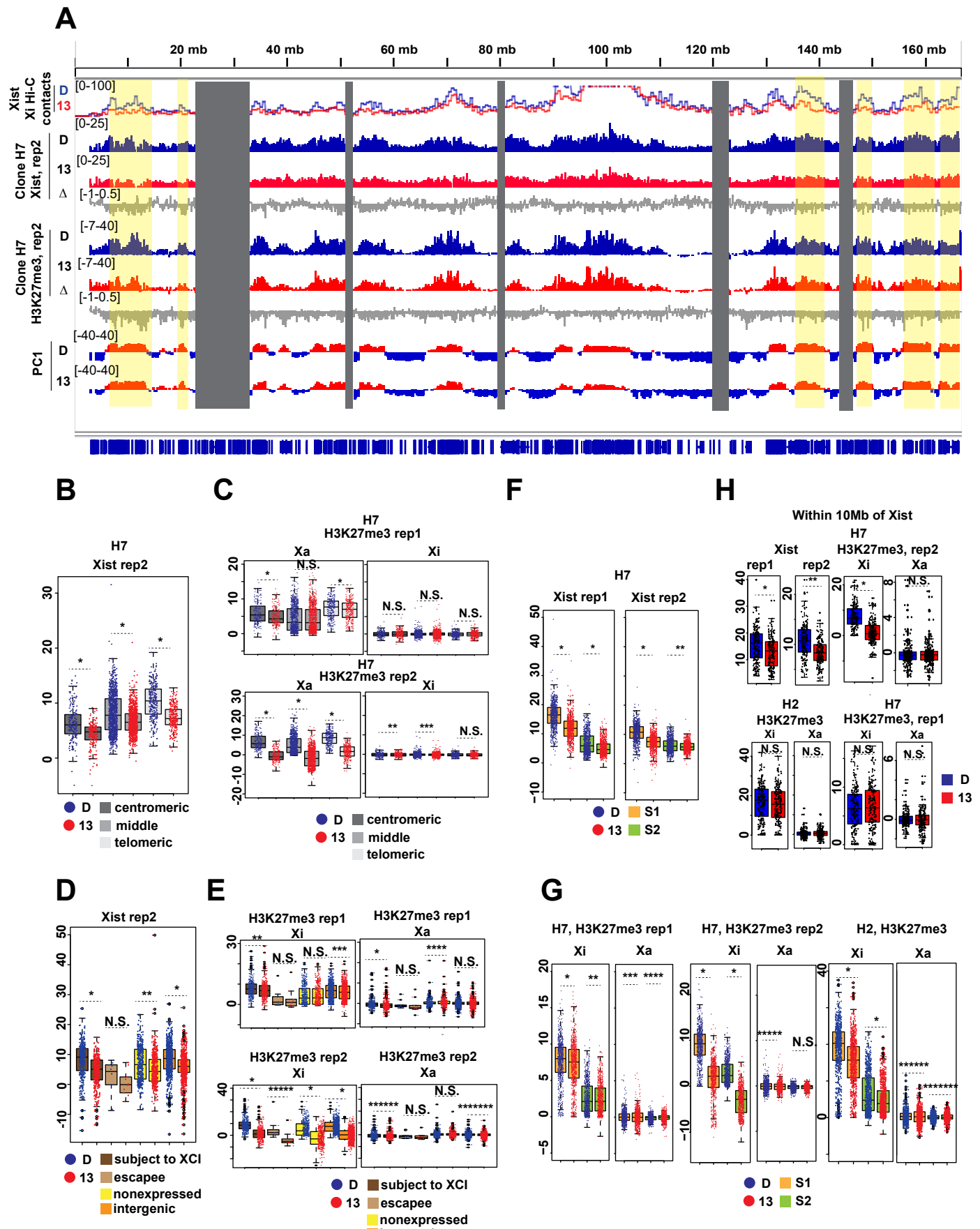


Figure S6